Proceedings of the ASME 2013 32nd International Conference on Ocean, Offshore and Arctic Engineering
OMAE 2013
June 9-14, 2013, Nantes, France

OMAE 2013-10509

LARGE EDDY SIMULATION OF FLOW PAST A STATIONARY AND CONTROLLED OSCILLATING CIRCULAR CYLINDER AT RE=5500

Sunghan Kim
Fluid Structure Interactions Group
University of Southampton, UK
Email: sunghan.kim@soton.ac.uk

Philip A. Wilson*
Fluid Structure Interactions Group
University of Southampton, UK
Email: philip.wilson@soton.ac.uk

Zhi-Min Chen
Fluid Structure Interactions Group
University of Southampton, UK
Email: z.chen@soton.ac.uk

ABSTRACT

Vortex shedding from a stationary cylinder and transversely oscillating circular cylinder in a uniform flow at a Reynolds number of 5500 is numerically studied by three-dimensional Large Eddy Simulation (LES). The filtered equations are discretised using the finite volume method with an O-type structured grid and a second-order accurate method in both time and space. Firstly, the main wake parameters of a stationary cylinder are examined and compared for different grid resolutions. Secondly, a transversely oscillating cylinder with a constant amplitude in a uniform flow is investigated. The cylinder oscillation frequency ranges between 0.75 and 0.95 of the natural Kármán frequency, and the excitation amplitude is 50% of the cylinder diameter. Comparisons with the available experimental data indicate that the present study has properly predicted the flow statistics of the cylinder wake for both the fixed and oscillating cylinder case, and numerically captured the vortex switching phenomenon, which is characterized by changes in forces and wake mode of shedding observed in the previous experiments at high values of Reynolds number.

INTRODUCTION

As the oil and gas field development activities have moved into deeper waters and areas of stronger ocean currents such as the Gulf of Mexico, the importance of vortex shedding on slender structures becomes more critical as there might result in serious engineering problems such as fatigue failure on offshore risers or clashing with each other. Therefore, the problem of a circular cylinder oscillating in the fluid has received a great deal of attention and the prediction of the fluid forces on a circular cylinder such as an offshore riser and subsea pipeline is of the primary tasks in the design of the structures. While the experimental and numerical studies of the flow around a circular cylinder has been the centre of various investigations over many years, it still remains a challenging task due to the complexity of the flow in the wake.

Several previous controlled or forced vibration studies exist in the literatures. [1] firstly investigated experimentally the forces exerted on a cylinder in a controlled oscillation over a wide range of frequencies and oscillation amplitudes. Their experiments showed that there was an abrupt change in the phase angle jump between the lift force and the cylinder motion when the frequency of oscillation is varied around the natural shedding frequency, which is called the synchronization condition.

A particular focus of the experiments on the controlled oscillating cylinder has been on the near wake with emphasis on excitation near synchronization. [2] performed experiments using the hydrogen bubble technique to study the timing of vortex shedding. [3] also conducted particle-imaging study of this timing problem at Re=185 and 5000. They found that some abrupt changes in flow topology and the phase between lift force and cylinder motion can be explained by a change of the timing of the vortices being shed. As the excitation frequency (f_e) increased per a small amplitude (A) and a given Reynolds number, the wake

*Tel: +44-(0)23-8059-3767 Address: Fluid Structure Interactions Research Group, Faculty of Engineering and the Environment, University of Southampton, Southampton, SO17 1BJ, UK.

vorticity moved closer to the cylinder, eventually reaching a limiting position and resulted in an abrupt switch of the vorticity concentration to the opposite side of the cylinder. This switching phenomenon occurred at both Re=185 and Re=5000 where small-scale Kelvin-Helmholtz (KH) vortices coexist with large-scale Kármán vortices.

In previous studies, the amplitude of oscillation was small and constant. [4] undertook forced oscillation experiments to identify the wake patterns with a range of amplitudes and a series of frequencies at Re=300 to 1000. They found a series of synchronization regions and the wake patterns in the regions were identified as 2S, 2P, P+S mode. [5] experimentally studied water flow past an elastically mounted circular cylinder (freely oscillating cylinder) and they observed the response behaviour is fairly similar to the forced oscillation experiments.

More recently, [6, 7] performed controlled oscillation experiments at Re=2300, 4100 and 9100 with various amplitude ratios. They defined a transition state (2P mode equivalent to the upper-branch of the freely oscillating cylinder) between two distinctly different wake states, the low frequency wake state (2P mode equivalent to the lower-branch of the freely oscillating cylinder) and high frequency wake state (2S mode equivalent to the initial-branch of the freely oscillating cylinder), as the excitation frequency passes through the natural frequency. They clearly showed that the transition state is also characterized by phase and lift jump together with wake mode and suggested that there are strong similarities in the wake structures between controlled oscillating and freely oscillating cylinder case.

Several recent numerical studies of the timing of vortex formation from forced oscillating cylinder have been performed. [8] numerically examined the forced oscillation problem at Re=185, 500 and 1000 and they used a finite difference method to simulate 2-D flow. They showed good agreements with the vortex switching phenomenon observed in the experiment at Re=185 by [3]. [9] performed 2-D simulation of in-line and cross-flow oscillating cylinder at Re=185, and found good agreements with numerical [8] and experimental [3] results. [10] performed 2-D direct numerical simulation (DNS) of controlled oscillating cylinder and validated that a change of the lift force on the oscillating cylinder was associated with a change in the timing of vortex. Recently, [11] conducted a 3-D DNS simulation of an oscillating circular cylinder at a high Reynolds number of 10000 and a moderate amplitude of oscillation. The drag and lift coefficient of the forced oscillation were predicted reasonably well compared with experimental data. However, the vortex structures in the wake were not presented at Re=10000. The 3-D effect on spanwise extension was investigated by [12] at various Reynolds numbers and their 3-D Large Eddy Simulation (LES) study stressed the importance of the proper spanwise extension required to predict accurately the flow around a circular cylinder. They suggested that πD as the minimum spanwise length is enough to capture the main wake parameters at high Reynolds number. [13] performed extensive 2-D LES of forced oscillating cylinder with a range of modulated excitation frequencies from Re=500 to 6000 and found good agreements with experimental results of wake modes. Recently,

The objective of the present study is to numerically examine the phenomenon of vortex switching from an oscillating circular cylinder observed in the experiments by [3, 7] at high Reynolds number. The influence of this vortex switching on time-dependent forces acting on the cylinder and changes in wake mode are examined. Comparisons with available experimental data are carried out.

COMPUTATIONAL MODEL AND PARAMETER

The incompressible 3-D turbulent flow past a circular cylinder is modelled in the frame of the Large Eddy Simulation (LES) approach using the time-dependent filtered Navier-Stokes equations.

The 3-D solution domain is shown in Figure 1. The cylinder axis is aligned with the spanwise direction (z) and the x-axis is along the stream-wise direction. The y-axis is cross-flow direction and orthogonal to the cylinder axis. A body-fitted and O-type structured grid is generated for this study. The hexahedral grid in the x-y plane is exponentially stretched in the radial direction (r) and is uniformly spaced in the circumferential direction (θ). The grid size is expressed as $r \times \theta \times z$ with outer boundary 15 cylinder diameters (D) from cylinder center and spanwise length is πD for all cases. Uniform flow U is imposed at the inflow without the disturbance level. The Neumann conditions are imposed at the outlet boundary. Periodic boundary conditions are employed at the spanwise ends of the cylinder to treat the cylinder as an infinitely long cylinder and to avoid the end wall effect.

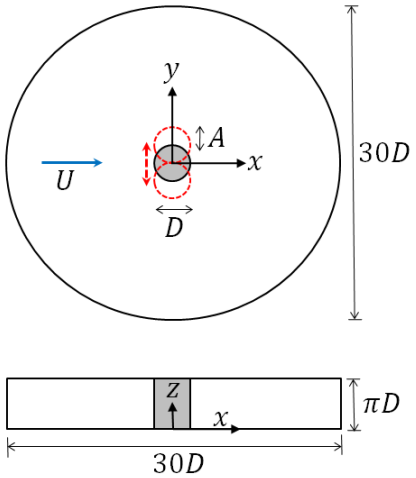

FIGURE 1. Geometric and computational domain.

The no-slip conditions are prescribed at the cylinder surface.

In the case of a cylinder oscillating transversely in a free stream, the cylinder motion $y(t)$ is given by the harmonic oscillation:

$$y(t) = Asin(2\pi f_e t) \quad (1)$$

with A and f_e as the oscillating amplitude and excitation frequency of oscillation respectively.

For modelling non-resolvable subgrid scales, the well known Smagorinsky type model is employed to represent the effects of the wake turbulence and all computations have been done with a Smagorinsky constant of C_s=0.1. The Van Direst damping formulation near cylinder wall is implemented and the non-dimensional normal distance from the wall (y^+) maintains around 1.0 throughout all simulation time.

Finite volume open source code OpenFoam [14] is used to evaluate the flow field. The governing equations are advanced in time using a second order implicit backward scheme and the spatial terms are discretised using the second-order central differencing (CD). The pressure-velocity coupling is achieved by the Pressure-Implicit with Splitting of Operators (PISO) algorithm. The constant time step of $\Delta tU/D = 0.002$ is used to maintain numerical stability. The flow data are gathered at least over $100U/D$ corresponding to approximately 21 vortex shedding cycles to obtain converged flow data.

APPLICATION AND RESULTS

The Fixed Cylinder

The simulations of the 3-D flow past a stationary cylinder are presented as a basis of comparison with experimental results for a complete validation of the LES simulation. The simulations were performed with different grid resolutions in the x-y plane and the spanwise z-direction. Adequacy of the near wall resolution in both planar and spanwise direction can be judged largely by the accuracy of force and pressure coefficients.

Table 1 summarizes the main wake parameters together with available experimental data. The Strouhal number $St = f_K D/U$ and the averaged drag coefficient $\bar{C}_D$ are generally in good agreements with the experimental data for all grid resolutions. However, the root-mean-square (r.m.s) of the lift coefficient C'_L shows a higher sensitivity to the different grid resolutions. With the low planar resolutions (case-A1, A2 and B1), C'_L generally lie at the upper bound of the experimental data at Re=6100 [15]. On the other hand, with the high planar mesh (case-C1 and D1) and the high spanwise mesh (case-B2), the statistic quantity tends to decrease to the lower bound of the experimental data at Re=5000 [15] and close to the empirical values at Re=5500 [15], which is about mean value of the experimental data [15]. Therefore, C'_L from the fine resolutions are predicted within the range

TABLE 1. Main wake parameters of stationary cylinder

Case ($r \times \theta \times z$)	St	$\bar{C}_D$	C'_L
A1 (160×160×64)	0.215	1.056	0.266
A2 (160×160×96)	0.215	1.082	0.309
B1 (180×180×64)	0.215	1.107	0.341
B2 (180×180×96)	0.215	1.048	0.243
C1 (200×200×64)	0.215	1.009	0.183
D1 (240×240×64)	0.215	1.042	0.233
Experimental data			
Re=5500 [15]	0.206	-	0.217
Re=5000-6100 [15]	0.209	-	0.15-0.27
Re=5500 [16]	-	1.05-1.10	

of experimentally measured values between Re=5000 and 6100, but somewhat higher than the value expected by empirical formula suggested by [15] at Re=5500. The small difference in r.m.s of fluctuating lift coefficient between experiment and simulation might be attributed to several influencing factors such as the free-stream turbulence level and the aspect ratio of the cylinder [17]. This study has allowed to determine a minimum grid size to obtain acceptable results and the best results compared to experiments are archived by case-B2 and case-D1. Considering computation time in LES simulation, the mesh of 180×180×96 (case-B2) is chosen for use in the next part of the present study.

Figure 2 shows the force coefficients for case-B2. The time

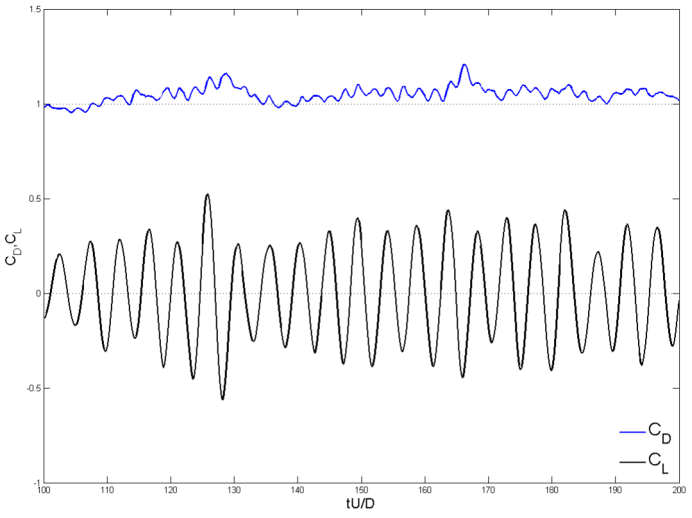

FIGURE 2. Time history of drag and lift coefficient (case-B2).

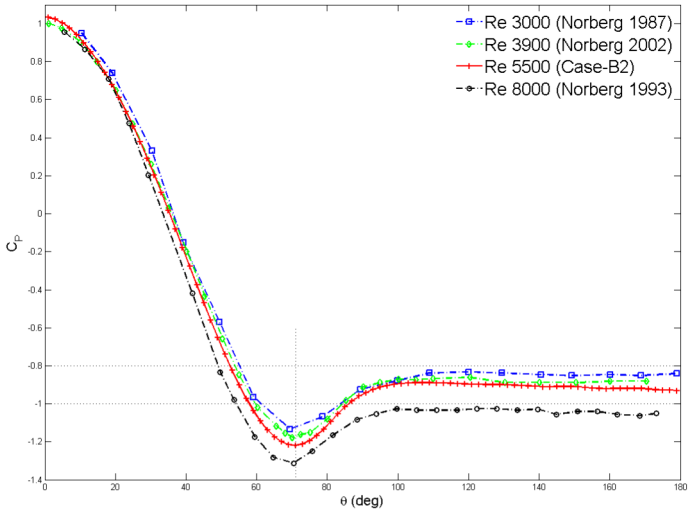

FIGURE 3. Mean pressure coefficient distribution (case-B2).

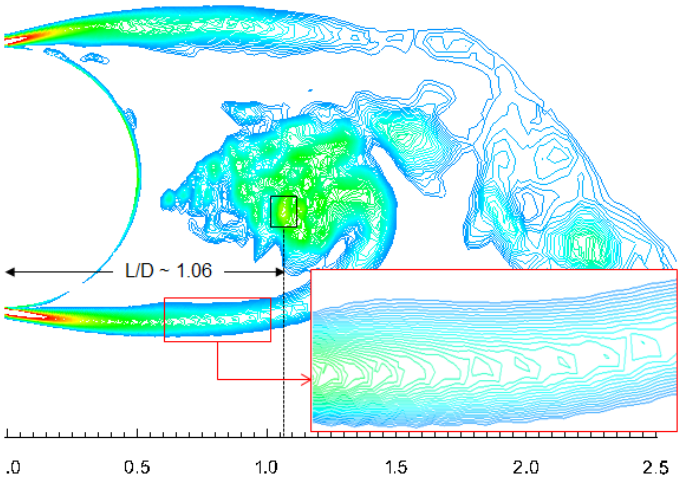

FIGURE 4. Instantaneous vorticity fields in x-y plane (case-B2): large-scale vortex and shear layer vortices in separated shear layers.

traces present the behaviour of the drag and lift coefficients with irregular amplitudes over time.

In Figure 3 the mean pressure distribution on the cylinder surface (case-B2) is examined and compared to reference experimental data at various Reynolds numbers as there are no available experimental data at $Re \approx 5500$. The angle (θ) was measured clockwise from the stagnation point. It shows overall agreement and well bounded with experiment results at upper and lower Reynolds numbers. Overall, Case-B2 seems to reasonably capture the mean pressure coefficient along the cylinder surface. After the point where the slope of the C_p curve changes ($\approx 71^\circ$), the behaviour of the pressure coefficient is similar to the curve at Re=3900 when compared to those at Re=3000 and 8000. The base pressure coefficient C_{Pb} =-0.93 obtained from case-B2 shows a fairly good agreement with the measured value of $C_{Pb} \approx$-0.95 [18]. These good agreements of the fluid forces and pressure on the stationary cylinder as shown in this section indicate that case-B2 with Smagorinsky type model should provide sufficiently converged solutions when the body is forced to oscillate as well.

The representative flow features at Re=5500 are shown in Figure 4 and Figure 5. Figure 4 shows a well defined large-scale vortex formed from the lower side of the cylinder. In the present study the length scale L/D for starting of the wake vortex is predicted as $\approx$1.06 and the length scale is slightly shorten than the experimental data (L/D$\approx$ 1.26) at Re=4800 [19]. Considering the fact that the formation length of wake is relatively long at $Re \leq$4000 and the length is severely shortened at Re=10000 [20], it seems that the length scale reasonably captures in the present LES study. The small-scale concentration of vorticity is shown embedded within the shear layers in close view as well. The simulation result shows that the shear layer vortices is not fully

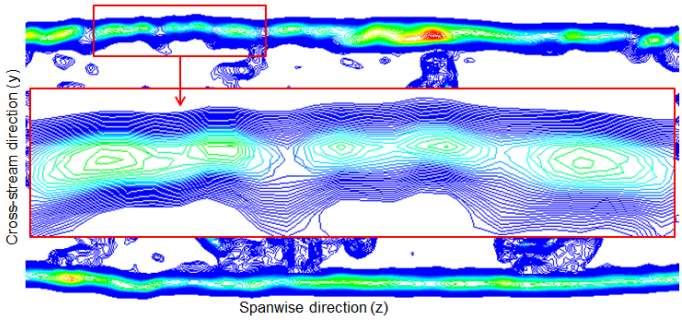

FIGURE 5. Instantaneous vorticity fields at $x/D = 0.625$ in y-z plane (case-B2): pairs of streamwise vortices in separated shear layers.

converged at Re=5500.

Figure 5 clearly shows repetitive streamwise vortices along spanwise direction in the separated shear layers prior to the formation of the large-scale vortex. These streamwise vortices are known to be superimposed on the spanwise shear layer vortices but no clear capture of the coalesce within the thin layers is predicted for the present study.

The Oscillating Cylinder

In this section, the turbulent flow past an oscillating circular cylinder in the cross-stream direction at Re=5500 is numerically examined to study the influence of the oscillating cylinder on the forces and the fundamental features of near wakes when the vortex switching occurs. Five different calculations were performed: five frequency ratios f_e/f_K=0.75, 0.80, 0.85, 0.90 and 0.95 with a constant amplitude ratio A/D=0.50. The terms A

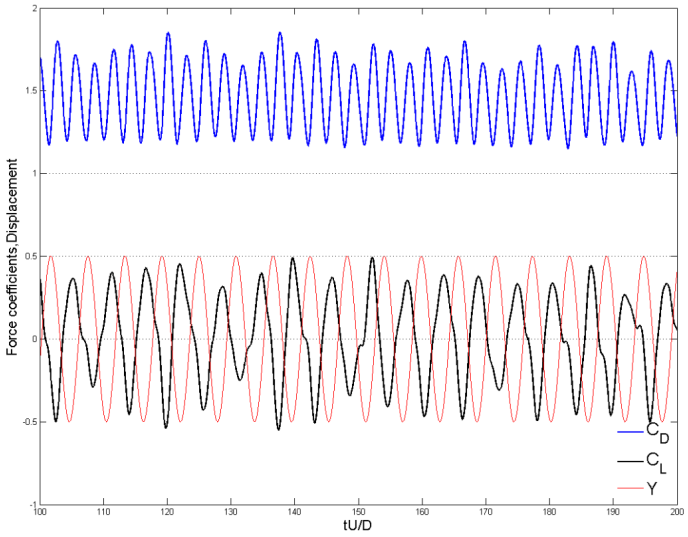

(a) f_e/f_K=0.80

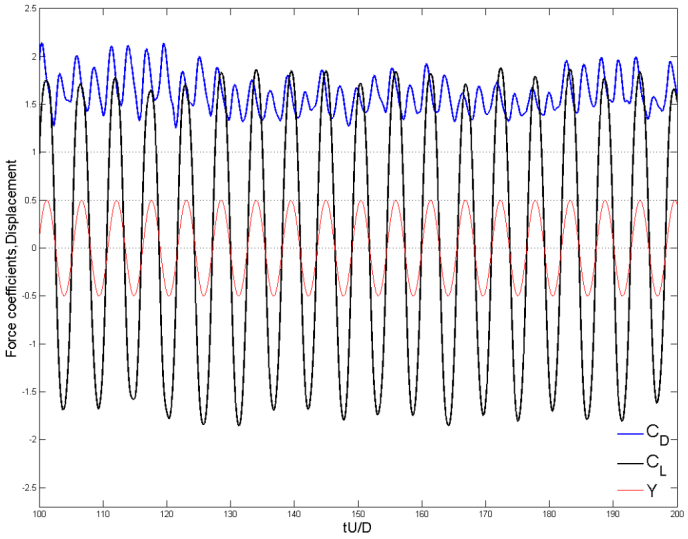

(b) f_e/f_K=0.85

FIGURE 6. Time history of the force coefficients and the cylinder displacement at Re=5500 and A/D=0.5.

and f_e were defined after equation (9) while f_K represents the Kármán frequency of the wake from a stationary cylinder. The parameters of the frequency ratios are based on the observations of [3] at Re=5000 with the goal of reproducing a close approximation of the experimental results measured by [3] and [7] at high Reynolds number.

Figure 6 shows the force coefficients and the cylinder displacement $y(t)$ for the frequency ratio f_e/f_K=0.80 and 0.85. At lower value of f_e/f_K=0.80, lift coefficient has small amplitude values of about 0.3 and time history of lift coefficient is approximately out-of-phase with the cylinder displacement. As f_e/f_K increases to 0.85 lift coefficient exhibits regular harmonic sign with a large amplitude of about 1.3 and the phase between lift and cylinder oscillation is approximately in-phase.

[7] clearly defined that these variations of the phase and amplitude of the lift coefficient represent a transition from a low-

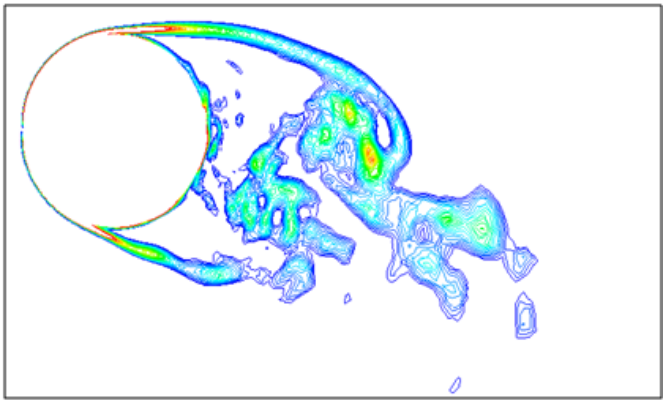

(a) Low-frequecy state at f_e/f_K=0.80; 8$\leq|\omega|D/U\leq$30, z/D=2.6.

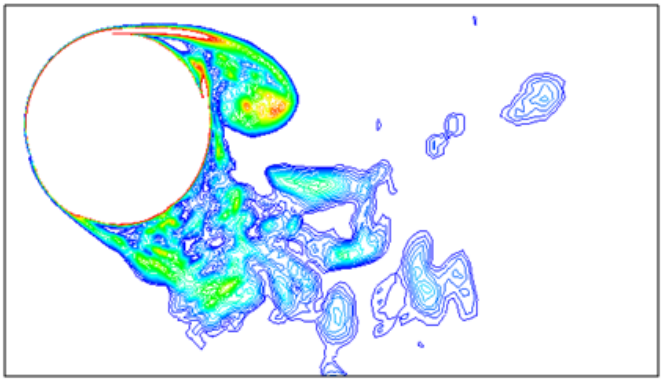

(b) High-frequency state at f_e/f_K=0.85; 6$\leq|\omega|D/U\leq$30, z/D=2.6.

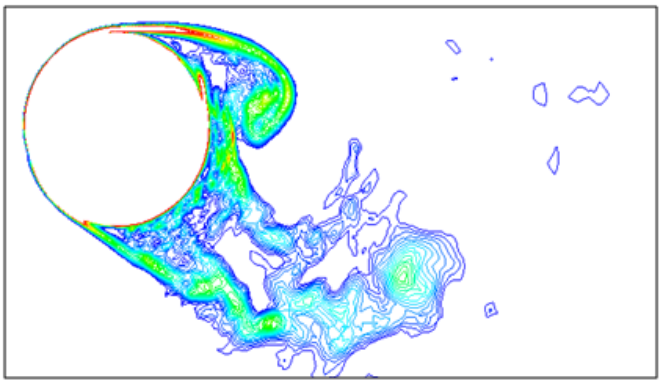

(c) High-frequency state at f_e/f_K=0.90; 6$\leq|\omega|D/U\leq$30, z/D=2.6.

FIGURE 7. Instantaneous vorticity magnitude at Re=5500 and A/D=0.5; The location of the cylinders is at its extreme upper position of the cylinder displacement for all cases.

frequency state to a high-frequency state with the corresponding the change of near wake structures and mode of shedding. The instantaneous vorticity fields in Figure 7 show two distinctly different near wake structures at the low and high-frequency state. The position of the cylinders is at the top of the cylinder oscillation and at z/D=2.6 in spanwise direction for all cases. Figure 7(a) is representative of the near wake structure at f_e/f_K=0.80 before transition while the amplitude of C_L is small and approximately out-of-phase with the cylinder oscillation. At this low-frequency state, the vortex structure of the upper side of the cylinder is formed from the attached shear layer and the length of the structure extends across the back of the cylinder. As f_e/f_K increases from 0.80 to 0.85 in high-frequency state, the initially elongated vortex structure attached the upper side of the cylinder moves closer to the cylinder base and reaches the limiting position while the amplitude of C_L becomes large and approximately in-phase with the cylinder oscillation at this high-frequency state. Whilst the upper vortex structure has rolled up tightly behind the cylinder, the streamwise length of the vortex structure of the lower side of the cylinder starts to extended to streamwise direction as f_e/f_K increases to 0.90. This vortex switching process is consistent with the experimental observation of [3].

The wakes of vortex shedding at low and high-frequency state generate significantly different modes downstream of the cylinder. Figure 8 shows the wake modes for low and high-frequency states. In Figure 8(a) the portion of vorticity at the end of upper negative shear layer is separated and forms a counter rotating pair with previously shed positive vorticity, which is com-

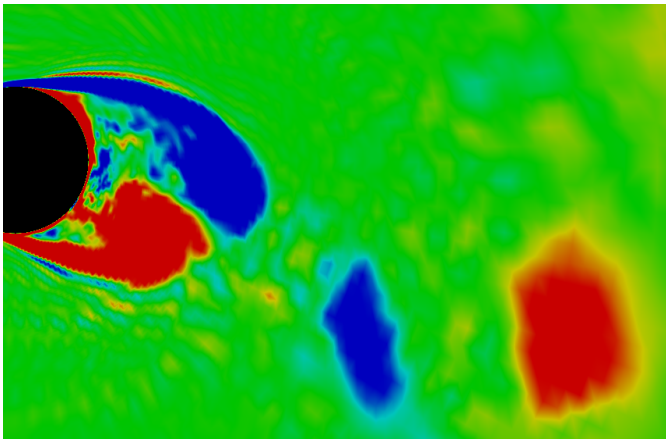

(a) Low-frequecy state at f_e/f_K=0.80 showing the 2P mode of shedding.

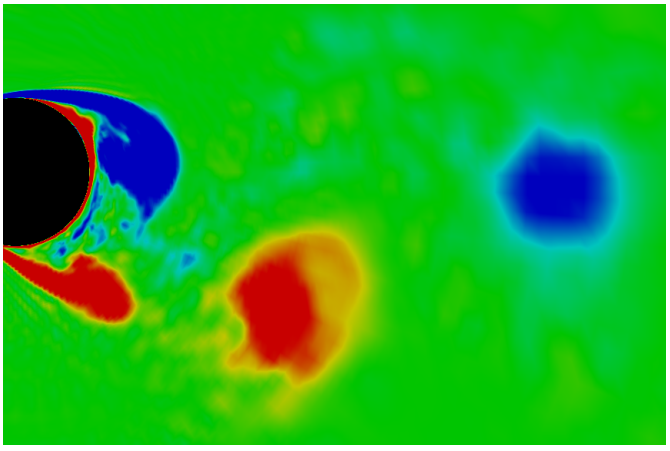

(b) High-frequency state at f_e/f_K=0.85 showing the 2S mode of shedding.

FIGURE 8. Phase averaged vorticity ω_z fields at Re=5500 and A/D=0.5; The location of the cylinders is at its extreme upper position of the cylinder displacement for all cases.

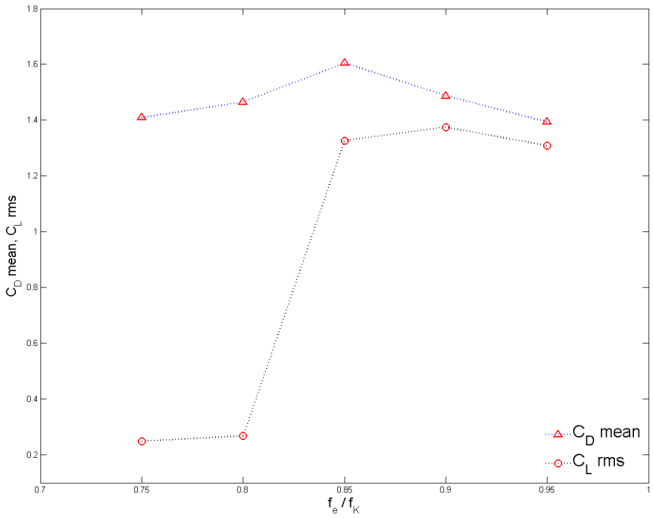

(a) $\bar{C}_D$ and C'_L

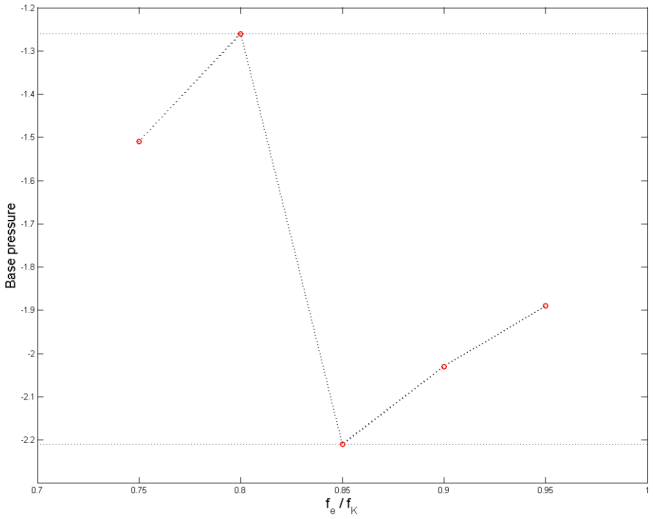

(b) The mean pressure coefficient variation.

FIGURE 9. Time-averaged values of force and pressure coefficient as a function of f_e/f_K at Re=5500 and A/D=0.5.

monly described as the 2P mode of shedding [4]. Figure 8(b) shows a single positive vortex is shed and separated, which is correspond to the 2S mode of shedding [4]. The present numerical study clearly shows that the average vorticity fields for the low and high-frequency correspond to the 2P and 2S mode of shedding respectively, and the numerical results are well consistent with recent experimental results measured by [7].

The time-average drag and r.m.s lift coefficients are shown in Figure 9(a) as a function of frequency ratios. The peak of the coefficients are in the range $0.80 \leq f_e/f_K \leq 0.90$. The r.m.s. values of the lift coefficients do not vary significantly until f_e/f_K=0.80 and show a sharp jump as f_e/f_K goes from 0.80 to 0.85. As f_e/f_K increases further, C_L' gradually changes. The sharp jump of the lift force has been observed in previous experimental studies. In the present numerical study, the phase jump of C_L' occurs at $0.80 < f_e/f_K < 0.85$ at *Re*=5500 and A/D=0.5, whereas experimentally [3], the vortex switching process involving the phase jump of the fluctuating lift was observed at $0.85 < f_e/f_K < 0.90$ at *Re*=5000 and relatively low amplitude ratio A/D=0.2. $\bar{C}_D$ does not vary strongly throughout transition and shows very similar magnitude either side of transition. Figure 9(b) shows the base pressure coefficient when the location of the cylinder is at its maximum positive position. The base pressure variation is seen to drop sharply between f_e/f_K=0.80 and 0.85 where vortex switching occurs, and gradually increase again.

CONCLUSIONS

The present study summarizes numerical results of three-dimensional large eddy simulations of the turbulent flow past a circular cylinder at *Re*=5500. Two configurations are investigated: a stationary cylinder and forced oscillating cylinder in cross-flow direction. The main wake parameters of a stationary cylinder are examined for the primary purpose of justifying the grid resolution. A comparison between the calculated and experimental results indicates that the flow quantities are correctly predicted, and small-scale vortices in the separated shear layers are numerically captured as well. The LES results for a stationary cylinder case generally agree well with experimental data.

The phenomenon of the vortex switching observed in the experiment at high Reynolds number is numerically reproduced at *Re*=5500. The instantaneous structures of the near wake of a cylinder subjected to forced oscillation is examined and the change of vortex structures is numerically observed at $0.80 < f_e/f_K < 0.85$. It is consistent with sharp changes in lift and base pressure coefficient. Therefore, this numerical study shows that the transition from low-frequency state to high-frequency state occurs at $0.80 < f_e/f_K < 0.85$. Moreover, the phase averaged vorticity fields clearly show the different wake modes either side of the transition, 2P and 2S mode of shedding. These numerical results are well consistent with the experimental results observed by [3, 7].

ACKNOWLEDGMENT

The authors acknowledge the financial support from Lloyd's Register Educational Trust. The computations were performed on the IRIDIS-3 high performance computing resources of the University of Southampton.

REFERENCES

[1] Bishop, R., and Hassan, A., 1964. "The lift and drag forces in a circular cylinder in a flowing fluid". *Proceedings of the Royal Society of London,* ***277***, pp. 32–48.

[2] Ongoren, A., and Rockwell, D., 1988. "Flow structure from an oscillating cylinder part 1. mechanisms of phase shift and recovery in the near wake". *Journal of Fluid Mechanics,* ***191***, pp. 197–223.

[3] Gu, W., Chyu, C., and Rockwell, D., 1994. "Timing of vortex formation from an oscillating cylinder". *Physics of Fluids,* ***6***, pp. 3677–3682.

[4] Williamson, C., and Roshko, A., 1988. "Vortex formation in the wake of an oscillating cylinder". *Journal of Fluids and Structures,* ***2***, pp. 355–381.

[5] Khalak, A., and Williamson, C., 1999. "Motions, forces, and mode transitions in vortex-induced vibrations at low mass damping". *Journal of Fluids and Structures,* ***13***, pp. 813–851.

[6] Carberry, J., Sheridan, J., and Rockwell, D., 2001. "Forces and wake modes of an oscillating cylinder". *Journal of Fluids and Structures,* ***15***, pp. 523–532.

[7] Carberry, J., Sheridan, J., and Rockwell, D., 2005. "Controlled oscillations of a cylinder: forces and wake modes". *Journal of Fluid Mechanics,* ***538***, pp. 31–69.

[8] Lu, X., and Dalton, C., 1996. "Calculation of the timing of vortex formation from an oscillating cylinder". *Journal of Fluids and Structures,* ***10***, pp. 527–541.

[9] Guilmineau, E., and Queutey, P., 2002. "A numerical simulation of vortex shedding from an oscillating circular cylinder". *Journal of Fluids and Structures,* ***16***, pp. 773–794.

[10] Blackburn, H., and Henderson, R., 1999. "A study of two-dimensional flow past an oscillating cylinder". *Journal of Fluid Mechanics,* ***385***, pp. 255–286.

[11] Dong, S., and Karniadakis, G., 2005. "Dns of flow past a stationary and oscillating cylinder at re=10000". *Journal of Fluids and Structures,* ***20***, pp. 519–531.

[12] Labbé, D., and Wilson, P., 2007. "A numerical investigation of the effects of the spanwise length on the 3-d wake of a circular cylinder". *Journal of Fluids and Structures,* ***23***, pp. 1168–1188.

[13] Atluri, S., Rao, V., and Dalton, C., 2009. "A numerical investigation of the near-wake structure in the variable fre-

quency forced oscillation of a circular cylinder". *Journal of Fluids and Structures,* ***25***, pp. 229–244.

[14] Weller, H., Tabor, G., Jasak, H., and Fureby, C., 1998. "A tensorial approach to cfd using object orientated techniques". *Computers in Physics,* ***12***, pp. 620–631.

[15] Norberg, C., 2003. "Fluctuating lift on a circular cylinder: review and new measurement". *Journal of Fluids and Structures,* ***17***, pp. 57–96.

[16] Khalak, A., and Williamson, C., 1996. "Dynamics of a hydroelastic cylinder with very low mass and damping". *Journal of Fluids and Structures,* ***10***, pp. 455–472.

[17] Breuer, M., 1998. "Numerical and modeling influences on large eddy simulations for the flow past a circular cylinder". *International Journal of Heat and Fluid Flow,* ***19***, pp. 512–521.

[18] Norberg, C., 1994. "An experimental investigation of the flow around acircular cylinder: influence of aspect ratio". *Journal of Fluid Mechanics,* ***258***, pp. 287–316.

[19] Kourta, A., Boisson, H., Chassaing, P., and Ha Minh, H., 1987. "Nonlinear interaction and the transition to turbulence in the wake of a circular cylinder". *Journal of Fluid Mechanics,* ***181***, pp. 141–161.

[20] Thompson, M., and Hourigan, K., 2005. "The shear-layer instability of a circular cylinder wake". *Physics of Fluids,* ***17,021702***, pp. 1–4.